0273-2289/02/101/0131/$15.25

Optimization of Glycerol Fed-Batch Fermentation in Different Reactor States

A Variable Kinetic Parameter Approach

Dongming Xie, Dehua Liu,* Haoli Zhu, and Jianan Zhang

Institute of Applied Chemistry, Department of Chemical Engineering, Tsinghua University, Beijing 100084, P.R. China, E-mail: dhliu@tsinghua.edu.cn

Received July 1, 2001; Revised November 1, 2001; Accepted November 1, 2001

Abstract

To optimize the fed-batch processes of glycerol fermentation in different reactor states, typical bioreactors including 500-mL shaking flask, 600-mL and 15-L airlift loop reactor, and 5-L stirred vessel were investigated. It was found that by reestimating the values of only two variable kinetic parameters associated with physical transport phenomena in a reactor, the macrokinetic model of glycerol fermentation proposed in previous work could describe well the batch processes in different reactor states. This variable kinetic parameter (VKP) approach was further applied to model-based optimization of discrete-pulse feed (DPF) strategies of both glucose and corn steep slurry for glycerol fed-batch fermentation. The experimental results showed that, compared with the feed strategies determined just by limited experimental optimization in previous work, the DPF strategies with VKPs adjusted could improve glycerol productivity at least by 27% in the scale-down and scale-up reactor states. The approach proposed appeared promising for further modeling and optimization of glycerol fermentation or the similar bioprocesses in larger scales.

Index Entries: Macrokinetic model; variable kinetic parameter; glycerol production; fed-batch fermentation; discrete-pulse feed strategy; reactor state.

Introduction

Glycerol production by fermentation using osmophilic yeast has been studied for decades in China to meet the great commercial demand *(1)*.

*Author to whom all correspondence and reprint requests should be addressed.

Considering that high glucose concentration leads to inhibition in the fermentation whereas low concentration reduces glycerol productivity, the fed-batch fermentation seems more efficient than the batch mode *(2)*. In addition, the high concentration ratio of the final glycerol to residual glucose in fed-batch process makes the process more attractive since it is more advantageous for glycerol recovery during the downstream distillation process *(3)*.

For optimization of glycerol fed-batch fermentation, the first difficulty is to optimize two kinds of feed operation at the same time since the key limited nutrients to be fed include both glucose and corn steep slurry *(4,5)*. Some previous works *(4–6)* have investigated the fed-batch process for glycerol production, in which both nutrients were fed in pulse form at certain time intervals to maintain glucose and/or cell concentration within a certain range and the feed schemes were obtained just by comparison of finite batches of experiments. However, these feed strategies were determined neither by analysis of biochemical mechanism nor by optimization strategy, and thus it was difficult to ensure that an optimal state was approached. To obtain more reliable feed strategies, both a physiologic model approach and a dynamic optimization were widely adopted *(7)*. The former needs precise description of the metabolic mechanisms, and, thus, is difficult to apply in many fermentation processes, while the latter generally comes down to a singular optimal control problem, which is difficult to solve by general numerical methods especially for glycerol fed-batch fermentation with two feed rates to be optimized *(2,8,9)*. To conveniently solve the optimization problem and apply the optimized feed schemes to practical process, recent work *(10)* proposed that the fed-batch process be divided into multiple equal subintervals and the nutrients be fed in pulse form at the start of each subinterval. The multipulse feed strategies were optimized by a steady-state nonlinear optimization approach. The strategies were verified by experiments in a 600-mL airlift loop reactor (ALR), and a higher glycerol productivity than suggested by Sun *(4)* and Yang *(5)* was achieved.

However, when the form, scale, and/or the operation mode of the reactor (i.e., reactor state) are significantly changed, the fermentation process usually becomes much different since the biochemical reaction relies so much on the physical transport characteristics in the reactor. Therefore, the new challenge is how to adjust the optimized feed strategies according to different reactor states. In fact, if a flexible kinetic model were developed to describe the bioprocesses in different reactor states, then the problem should be conveniently solved by model-based optimization.

In the present study, few of the kinetic parameters of the macrokinetic model proposed in ref. *2*, which reflected the physical transport characteristics in the reactor, were identified as variable ones. By adjusting values of the variable kinetic parameters (VKPs), the macrokinetic model was first attempted to simulate glycerol batch fermentation in 500-mL shaking flask, and 600-mL and 15-L ALRs, respectively. Based on the simulation results,

the VKP approach was further applied to optimize discrete-pulse feed (DPF) strategies proposed in a previous study *(10)* for glycerol fed-batch fermentation and verified experimentally in a scale-down process in a 500-mL shaking flask and a scale-up process in a 5-L stirred vessel.

Macrokinetic Model of Glycerol Fermentation

General Model Equations

In previous work *(2)*, a kinetic model for glycerol production by batch fermentation with the osmophilic yeast *Candida krusei* at constant 35°C was investigated. The growth model was represented by Eq. 1, in which the key culture factors, including cell viability attenuation with culture time, oxygen promotion to growth, limitation of both glucose and phosphorus content, and inhibition of glucose were considered:

$$\frac{dX}{dt} = \mu_{max} \cdot \exp\left(-\frac{t}{k_t}\right) \cdot \left(1 + \frac{K_O}{1 + X/K_{do1}}\right) \cdot \frac{S}{(K_{S1}X + S)\,(1 + S^2/K_{IS})} \cdot \frac{Ph}{K_{Ph1} + Ph} \cdot X \quad (1)$$

in which X, S, and Ph are the concentrations of cell, glucose, and phosphorus, respectively; t is the culture time; K_t, K_O, K_{do1}, K_{S1}, K_{IS}, and K_{Ph1} are the kinetic parameters for the growth equation.

By modifying the traditional kinetic models of nutrient uptake and product accumulation *(11)*, Eqs. 2 and 3 were applied to describe kinetics of glucose uptake and glycerol production, respectively:

$$-\frac{dS}{dt} = \begin{cases} \dfrac{1}{Y_{X/S}} \cdot \dfrac{dX}{dt} + \dfrac{m_t S}{K_{SP}P + S} \cdot \dfrac{Ph}{K_{Ph2} + Ph} X + \dfrac{1}{Y_{P/S}} \cdot \dfrac{dP}{dt}; & t \geq t_d \\ 0; & t < t_d \end{cases} \quad (2)$$

$$\frac{dP}{dt} = \alpha\frac{dX}{dt} + \beta\frac{S_0}{(1 + X/K_{do2})^2} \cdot \frac{Ph}{K_{Ph3} + Ph} X - \frac{K_{SP}P}{K_{SP}P + S} \cdot \frac{Ph}{K_{Ph2} + Ph} m_t X \quad (3)$$

in which P is the glycerol concentration; t_d is the delay time for glucose uptake; $Y_{X/S}$, m_t, K_{SP}, $Y_{P/S}$, α, β, K_{do2}, K_{Ph2}, and K_{Ph3} are the kinetic parameters. Phosphorous limitation of both glucose uptake and glycerol production, energy maintenance supplied by both glucose and glycerol, and oxygen promotion to glycerol production were also considered in Eqs. 2 and 3.

Considering that the phosphorous content is decreased mainly during the growth stage and that higher glucose concentrations lead to greater phosphorous uptake rate, a model for the phosphorous uptake was suggested by Eq. 4:

$$-\frac{dPh}{dt} = \frac{1}{Y_{X/Ph}} \cdot \frac{S^2}{K_{S2} + S^2}\frac{dX}{dt} \quad (4)$$

in which $Y_{X/Ph}$ is the yield coefficient of cell production based on phosphorus consumed, and K_{S2} is the saturation constant for glucose for phosphorous uptake.

Variable and Invariable Parameters of Macrokinetic Model

The biokinetics may be expressed at five different system levels *(11)*: molecular level model, single-cell model, population model, bioreactor model (bioprocess kinetics), and bioplant model. Generally, in the former three types of kinetics, all parameters of the mathematical model are strictly determined by biochemical mechanism or other biologic characteristics and thus are invariable and of exact values. However, the model applied herein belongs to the bioreactor model of macrokinetics; when the form, scale, or operation mode of the reactor (reactor state) is greatly changed, mass transfer processes of oxygen and nutrients and consequently the fermentation process may also be changed. To fit the new bioprocess curves, it is necessary to adjust the values of some kinetic parameters, but it is not necessary that all parameters be reestimated.

It was also assumed that parameters of the macrokinetic models could be classified into two groups. One group is associated basically with the inherent biochemical mechanism. It reflects the microscopic characteristics of the microbial reaction and cannot be influenced by the macroscopic physical transport process; thus, it can be called an *invariable kinetic parameter*. Another group is dependent not only on the microbial reaction mechanism, but also on the transport phenomena in the reactor, which must be influenced by the change of the reactor state; therefore, it can be called variable kinetic parameter (VKP). This means only VKPs of the macrokinetic model should be adjusted as the reactor state is significantly changed.

For the macrokinetic model of glycerol fermentation discussed here, the parameters K_{do1} and K_{do2} reflect the oxygen transfer state and may be changed with the variation in reactor state; therefore, they should be considered as *variable parameters*. In addition, K_{do1} and K_{do2}, according to ref. 2, reflected in essence the same oxygen transfer process; thus, the ratio of (K_{do1}/K_{do2}) was proposed constant no matter how the two parameters were changed:

$$(K_{do2}/K_{do1})_{\text{Reactor State (1)}} = (K_{do2}/K_{do1})_{\text{Reactor State (2)}} \tag{5}$$

In addition, corn steep slurry, as the main source of phosphorus, cannot be dissolved immediately or completely like glucose and is dispersed into microparticles or small lumps in the fermentation broth. When the reactor state was changed significantly, the mass transfer rate of phosphorus, from small particle or lump to the yeast cell, should also be changed. Therefore, even if the macroscopic phosphorous content in the fermentation liquor was kept at the same level, the effects of phosphorus on the fermentation should also be changed with the variation in reactor state and embodied in the variations of values of K_{Ph1}, K_{Ph2}, and K_{Ph3} in Eqs. 1–3. Then,

K_{Ph1}, K_{Ph2}, and K_{Ph3} were considered as the other *variable parameters*. Furthermore, the ratios of (K_{Ph1}/K_{Ph2}) and (K_{Ph1}/K_{Ph3}) were also assumed constant at any reactor state:

$$(K_{Ph2}/K_{Ph1})_{\text{Reactor State (1)}} = (K_{Ph2}/K_{Ph1})_{\text{Reactor State (2)}} \tag{6}$$

$$(K_{Ph3}/K_{Ph1})_{\text{Reactor State (1)}} = (K_{Ph3}/K_{Ph1})_{\text{Reactor State (2)}} \tag{7}$$

Then, by only reestimating the *variable parameters* of K_{do1} and K_{Ph1} (K_{do2}, K_{Ph2}, and K_{Ph3} are adjusted according to Eqs. 5–7), the model Eqs. 1–4 could be flexibly used to simulate the new fermentation process in a different reactor state.

Formulation of Fed-Batch Optimization Problem

The problem discussed here is to plan the pulse-feeding amounts in all subintervals as a whole to maximize the final glycerol yield while controlling the residual glucose at a low concentration so that glycerol can be efficiently separated from the reaction mixture during the downstream distillation process. Different from the dynamic optimal control strategy, here the control problem will be converted to a static optimization and solved by a general constrained global optimization approach. It must contain the following key factors.

State Equations (Bioprocess Model)

The state equations should be the kinetic model, Eqs. 1–4. For discrete-pulse fed-batch fermentation discussed here, the following mass balance should be considered between any two closest subintervals:

$$\left.\begin{aligned}
V_{0,i} &= V_{f,i-1} + V_{FS,i} + V_{FPh,i} \\
X_{0,i} &= X_{f,i-1} \cdot (V_{f,i-1}/V_{0,i}) \\
S_{0,i} &= (V_{f,i-1} \cdot S_{f,i-1} + V_{FS,i} \cdot S_{FS})/V_{0,i} \\
P_{0,i} &= P_{f,i-1} \cdot (V_{f,i-1}/V_{0,i}) \\
Ph_{0,i} &= (V_{f,i-1} \cdot Ph_{f,i-1} + V_{FS,i} \cdot Ph_{FS} + V_{FPh,i} \cdot Ph_{FPh}/V_{0,i})
\end{aligned}\right\} \tag{8}$$

in which the subscript i is the sequence number of the subinterval ($1 \le i \le N$); S_{FS} and Ph_{FS} are, respectively, the concentrations of glucose and phosphorus in the glucose feed tank; Ph_{FPh} is the phosphorous concentration in the feed tank of corn steep slurry (phosphorous source); and V_{FS} and V_{FPh} are feed volumes of glucose and corn steep slurry, respectively. Then by the Runge-Kutta method, the final glycerol and glucose concentration (P_f, S_f) can be obtained by integrating Eqs. 1–4 in sequence of the subintervals combined with Eqs. 8, and $P_f = P_{f,N}$; $S_f = S_{f,N}$.

Variables to Be Optimized

If the process is divided into N subintervals, then total $2N$ variables, including the feeding volumes of glucose ($V_{FS,1}$, $V_{FS,2}$, …, $V_{FS,N}$) and corn

steep slurry ($V_{FPh,1}$, $V_{FPh,2}$, …, $V_{FPh,N}$) at the start of all subintervals, should be optimized.

Constraint Conditions

First, the working volume should be limited within the maximum reactor capacity mainly by controlling the total feed amount of glucose ($V_{FS,\max}$); therefore,

$$0 \le \sum V_{FS,i} \le V_{FS,\max} \qquad (1 \le i \le N) \tag{9}$$

in which $V_{FS,i}$ is the feed volume of glucose at the start of the ith subinterval.

Second, since high glucose concentration in the final reaction mixture must lead to difficulty in the downstream glycerol recovery process, a further end point constraint *(10)* is suggested so that the concentration of residual glucose can be controlled under an upper limit, S_{end}, which was set as 2% (w/v) in this study:

$$S_f \le S_{end} \tag{10}$$

Finally, to avoid significant inhibition, the process concentration of glucose (S) should be constrained below an upper limit (S_{up}); thus, according to ref. *2*, another path constraint should be adopted:

$$0 \le S \le S_{up} = 40 \tag{11}$$

Objective Function

The objective is to maximize the final glycerol yield subject to constraints (Eqs. 9–11). The constraint conditions may be satisfied indirectly by adding a penalty function into the objective function *(12,13)*. Thus, the following objective functions (Eq. 12) should be minimized:

$$\begin{aligned} &J[(V_{FS,1}, V_{FS,2}, \ldots, V_{FS,N}), (V_{FPh,1}, V_{FPh,2}, \ldots, V_{FPh,N})] \\ &= -V_f \cdot P_f + fpen(V_{FS}) + fpen(S_f) + \int_0^{t_f} fpen(S) \cdot dt \end{aligned} \tag{12}$$

in which $fpen(V_{FS})$, $fpen(S)$, and $fpen(S_f)$ are the penalty functions, respectively, for constraint conditions (Eqs. 9–11). They can be determined, respectively, by:

$$fpen(V_{FS}) = \begin{cases} pen_{VFS} \cdot \left[\sum_{i=1}^{N} (V_{FS,i}) - V_{FS,\max} \right]^2 & \sum_{i=1}^{N} (V_{FS,i}) > V_{FS,\max} \\ 0 & \sum_{i=1}^{N} (V_{FS,i}) < V_{FS,\max} \end{cases} \tag{13}$$

$$fpen(S_f) = \begin{cases} pen_{sf} \cdot (S_f - S_{end})^2 & S_f > S_{end} \\ 0 & S_f \le S_{end} \end{cases} \quad (14)$$

$$fpen(S) = \begin{cases} pen_s \cdot (S - S_{up})^2 & S > S_{up} \text{ or } S < 0 \\ 0 & 0 \le S \le S_{up} \end{cases} \quad (15)$$

In Eqs. 13–15, pen_{VFS}, pen_{Sf}, and pen_S are coefficients for corresponding penalty functions; they were set as 0.1, 1, and 1, respectively, since at these values the numerical experiences showed that the maximum positive relative deviations from the set points of V_{FS}, S_f, and S_{up} could be ensured less than 1, 5, and 5%, respectively, which are sufficient in practical control processes.

Numerical Method

A constrained global optimization approach, Complex method of Box *(12,14,15)*, was performed to determine the DPF schemes. Based on previous experience *(2,10)*, a value >6 for total number of subintervals (N) is generally suitable for this kind of optimization problem, since at this value the numerical solution by the Complex method is relatively timesaving, and the final glycerol yield (P_f) obtained by this method is decreased by 5% at most compared with that by dynamic optimization with a conjugate gradient method. Therefore, the DPF strategy obtained by the constrained global optimization approach can be considered as a suboptimal fed-batch control.

Materials and Methods

Microorganism and Media

The osmophilic yeast *C. krusei* (ICM-Y-05), mainly producing glycerol during aerobic cultivation, was obtained from State Key Lab of Biochemical Engineering, Institute of Chemical Metallurgy, Academia Sinica. The composition of the media for seed culture was (analytical grade, Beijing Chemical) 10% (w/v) glucose; 0.3% (w/v) urea (analytical grade, Beijing Chemical); 0.3% (w/v) corn steep slurry (Yiyang Biochemical, Hunan Province, China); and for batch and fed-batch fermentation, 20–40% (w/v) glucose, 0.3% (w/v) urea, and 0.15–0.45% (w/v) corn steep slurry. All kinds of media were sterilized at 120°C for 20 min before any culture process.

Batch and Fed-Batch Fermentation in Four Reactor States

Seed was precultured aerobically for 12 h and then was inoculated into the culture media at a ratio of 10% (v/v). To investigate the effects of the form, scale, and operation mode of the bioreactor on the macrokinetics,

four typical reactor states were applied to batch and fed-batch experiments of glycerol fermentation (see Table 1). Since a pH within 3.0–5.0 had no significant effect on glycerol fermentation *(3,16)*, only the initial pH was adjusted to 4.5 by the addition of 1 *N* HCl. The pH in later processes could be kept by the yeast within 3.0–4.0 without the addition of any alkali or acid solution. During fed-batch fermentation, dry glucose powder and solution of corn steep slurry (10% [w/v]), based on the numerical results obtained by constrained global optimization, were fed instantly in pulse form at the start of each subinterval. The culture temperature was controlled at (35 ± 1)°C.

Additionally, all comparative experiments under certain culture conditions were performed in duplicate and in parallel. Since most of the errors in the data between any duplicate experiments were <5% and the maximum error was <10%, only the average values of the duplicate experiments were used.

Analytical Methods

More than 3 mL of fermentation broth was sampled during each sampling operation. First, 1 mL of fresh sample was diluted to 5–100 mL so that the cell number in the diluted sample could be controlled within (0.5–2) × 10^7 cells/mL, which is convenient for cell numeration analysis. The total cell number was determined by microscopic observation using a hemacytometer. Second, another 1-mL fresh sample was diluted to 50 mL, about 10 mL of the diluted sample was centrifuged at 2000 rpm (*g*-force > 4 kgf) for 5 min, and then 5 mL of centrifuged diluted sample was used for glycerol analysis and 4 mL for glucose analysis. Glycerol concentration was determined by the periodate-chromotropic acid analysis, and glucose concentration was obtained by Fehling's test *(17,18)*. Finally, the rest of the fresh sample was centrifuged at 3000 rpm (*g*-force > 2 kgf) for 5 min to separate the yeast for phosphorous analysis. Phosphorus (mainly in organic form) was converted into inorganic form at first by adding concentrated sulfuric acid and perhydrol, and then its concentration was determined by ammonium molybdophosphate analysis *(19)*.

Results and Discussion

Model Fitting of Glycerol Batch Fermentation in Different Reactor States

In a previous study *(2)*, three batch experiments at 35°C were conducted in a 600-mL ALR (i.e., reactor state [1] in Table 1) to verify the macrokinetic model (Eqs. 1–4). To broaden the applicability of the model in different compositions of culture media, initial glucose was investigated within 20–40% (w/v) while phosphorous content was changed within 40–120 μg/mL by controlling the concentration of corn steep slurry at a range

Table 1
Four Typical Reactor States for Batch and Fed-Batch Experiments

Reactor state	Reactor form	Scale	Working volume	Aeration rate (vvm)	Other characteristics
(1)	ALR	600 mL	400–480 mL	2.0	With draft tube to form internal loop flow
(2)	Shaking flask	500 mL	50–60 mL		With four layers of gauze and rotary speed of 160 rpm
(3)	ALR	15 L	10–12 L	1.5	With draft tube to form internal loop flow
(4)	Stirred vessel (BioStat B5, BBI)	5 L	3.0–3.6 L	1.5	With stirred speed of 400 rpm

Table 2
Values of Invariable Kinetic Parameters in Eqs. 1–4

Parameter	Value
μ_{max} (h^{-1})	111.0
K_t (h)	33.96
K_O (—)	2.174
K_{S1} (g/10^{10} cells)	652.3
K_{IS} (g/100 mL)^2	93.20
$Y_{X/S}$ (10^{10} cells/g)	1.625
m_t (g/10^{10} cells)	0.05924
K_{SP} (—)	0.192
$Y_{P/S}$ (g/g)	0.4793
α (10^{-10} g/cell)	0.0231
β (10^{-8} mL/[cell·h])	1.061E-03
$Y_{X/Ph}$ (10^8 cells/μg)	0.0545
K_{S2} (g/100 mL)^2	152.7

of 0.15–0.45% (w/v). All parameters were estimated by the Complex method of Box *(14,15)* to minimize the residual sum of squares between all experimental and simulated data. The estimated values of invariable kinetic parameters are listed in Table 2, and those of VKPs are listed in the row of reactor state (1) in Table 3. Comparison of the experimental data and corresponding model simulations is shown in Fig. 1, from which a good model fitting can be found.

Three batches of experiments in a 500-mL shaking flask reactor (reactor state [2] in Table 1) and one in a 15-L ALR (reactor state [3] in Table 1) were used to test further the applicability or flexibility of the model in different reactor states. Considering that the fermentation process usually becomes much different when the reactor state is significantly changed, here values of the VKPs, K_{do1}, and K_{Ph1} in reactor states (2) and (3) were also reestimated by the Complex method of Box *(14)* to minimize the residual sum of squares between the experimental and simulated data, during which K_{do2}, K_{Ph2}, and K_{Ph3} were adjusted by Eqs. 5–7. Figures 2 and 3 show that, in the new reactor states (2) and (3), the model simulations with VKPs adjusted still fit the experimental results very well. In addition, Fig. 3 shows that this fitting situation was much better than that without this treatment (i.e., K_{do1}, K_{do2}, K_{Ph1}, K_{Ph2}, and K_{Ph3} still took the values as in reactor state [1]). This suggested that, by adjusting values of the VKPs, which are associated closely with turbulence and physical transport processes in the bioreactor, the macrokinetic model could describe well the new glycerol fermentation processes when the form, scale, or operation state of the reactor was significantly changed.

Table 3
Values of VKPs in Three Typical Reactor States

Reactor state (form, working volume, aeration)	Value of VKP				
	K_{do1} (10^8 cells/mL)	K_{do2} (10^8 cells/mL)	K_{Ph1} (μg/mL)	K_{Ph2} (μg/mL)	K_{Ph3} (μg/mL)
(1) 600-mL ALR, 420 mL, 2 vvm	1.998	11.39	163.6	14.38	1.088
(2) 500-mL shaking flask, 50 mL, 160 rpm, and four layers of gauze	2.225	12.68	146.01	12.84	0.9707
(3) 15-L ALR, 10 L, 1.5 vvm	12.05	68.64	133.7	11.75	0.8888

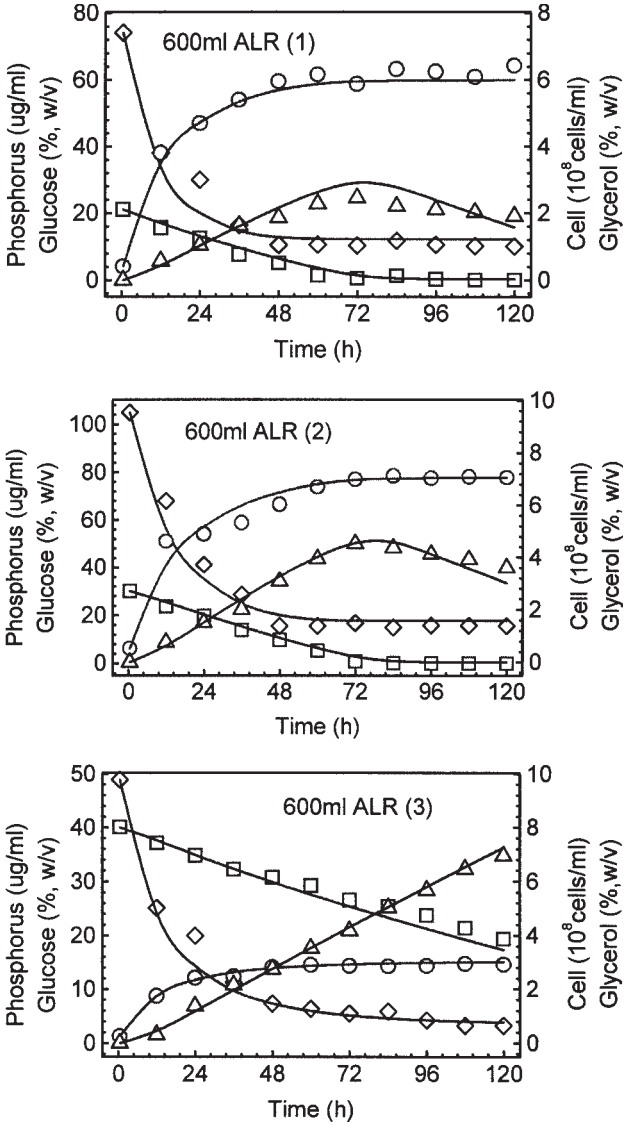

Fig. 1. Comparison between experimental data (○, cell; □, glucose; △, glycerol; ◇, phosphorus) and corresponding model simulations (solid lines) in 600-mL ALR (450 mL, 2 vvm).

Fig. 2. *(opposite page)* Comparison between experimental data (○, cell; □, glucose; △, glycerol; ◇, phosphorus) and corresponding model simulations with VKPs adjusted (solid lines) in 500-mL shaking flask (50 mL, 160 rpm, and four layers of gauze).

Fig. 3. *(opposite page)* Comparison between experimental data (○, cell; □, glucose; △, glycerol; ◇, phosphorus) and corresponding model simulations with VKPs adjusted (solid lines) or without this treatment (dotted lines) in 15-L ALR (10 L, 1.5 vvm).

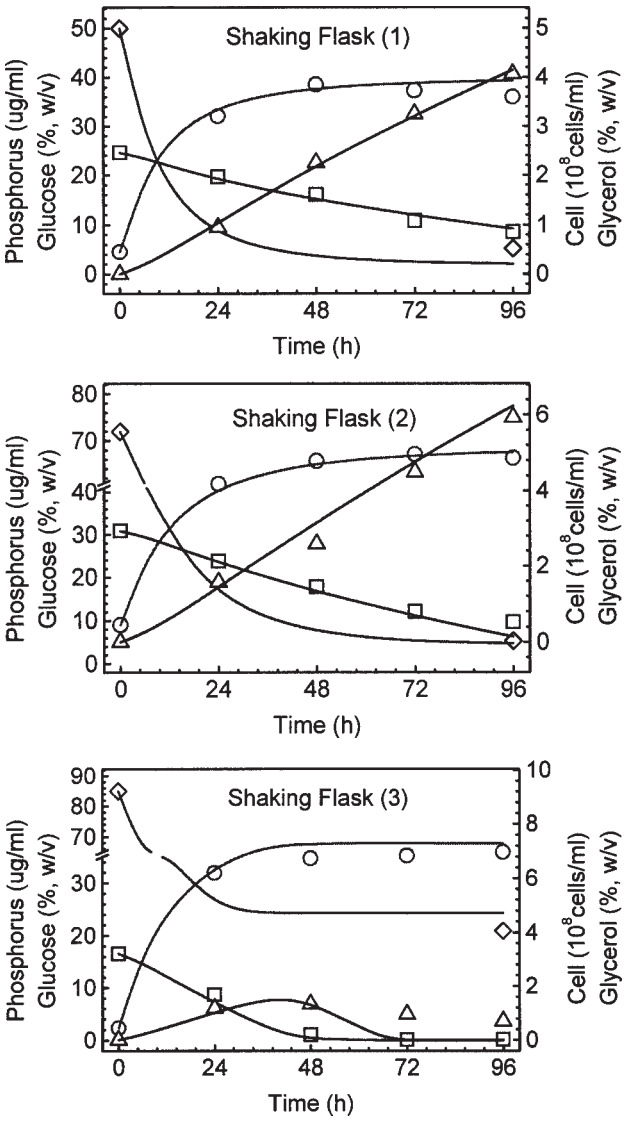
Shaking Flask (1)
Shaking Flask (2)
Shaking Flask (3)
Phosphorus (ug/ml)
Glucose (%, w/v)
Cell (10^8cells/ml)
Glycerol (%, w/v)
Time (h)

Fig. 2

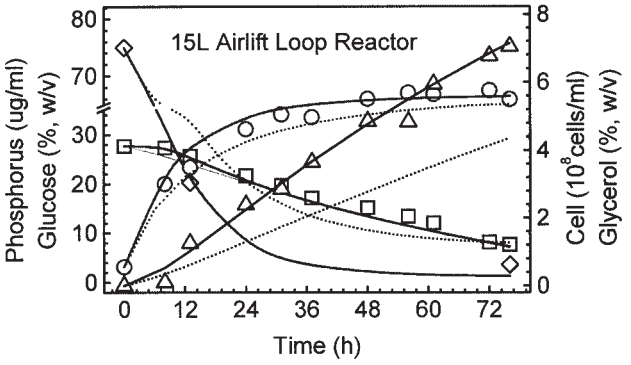
15L Airlift Loop Reactor
Phosphorus (ug/ml)
Glucose (%, w/v)
Cell (10^8cells/ml)
Glycerol (%, w/v)
Time (h)

Fig. 3

Optimization of Glycerol Fed-Batch Fermentation in Different Reactor States

In a previous study *(10)*, the DPF strategy (i.e., multipulse feed strategy in ref. *10*) in reactor state (1) optimized by the nonlinear approach was compared experimentally with the strategies of Sun *(4)* and Yang *(5)*, which were determined just by comparisons of multiple batches of experiments at various traditional feed schemes. In Sun's strategy *(4)*, dry glucose powder was fed with 24 g every 24 h during h 24–144, and corn steep slurry was fed with 0.14 mL every 24 h during h 24–144 and with 0.07 mL every 24 h during h 144–216. In Yang's strategy *(5)*, glucose was fed after h 24 to maintain the glucose concentration at 25–30%, and corn steep slurry was fed with 0.14 mL every 24 h during h 72–168 and with 0.07 mL every 24 h during h 168–216. It was found that, among the three kinds of feed operations, the DPF strategy determined by the model-based nonlinear optimization had the highest glycerol productivity, and the strategy of Yang *(5)* had the second highest. Since the VKP approach discussed in the previous section made the macrokinetic model exhibit a good applicability for glycerol batch fermentation in various reactor states, it was further used to optimize the DPF strategies in a scale-down process in reactor state (2) and a scale-up process in reactor state (4).

For reactor state (1) discussed in Xie et al. *(10)* or for reactor state (2) discussed herein, the VKPs still took the values as shown in Table 3. However, this does not mean that values of the VKPs in any new reactor state must be known *a priori* or reestimated based on previous experiments before any model-based application. In fact, if the reactor state could result in relatively drastic turbulence and good oxygen transfer in broth, then the glycerol fermentation process at such a reactor state must appear relatively stable. It has always been found that, when the reactor scale was larger than 5 L and the aeration rate was higher than 1.5 vvm, almost no deviations >10% at dynamics of cell growth, substrate uptake, and product formation could result from the reactor state variation *(2,3)*. Therefore, in the present study, we only used the VKP values in reactor state (3) to optimize the fed-batch process in reactor state (4).

The numerical conditions for the optimizations were as follows: S_0 = 30%; $X_0 = 0.55 \times 10^8$ cells/mL; $P_0 = 0\%$; $Ph_0 = 60\,\mu g/mL$; $S_{FS} = 1.8$ g/mL (glucose was also fed in dry powder form in this study; therefore S_{FS} could be considered as the density of dry glucose); $Ph_{FS} = 0\ \mu g/mL$; $Ph_{FPh} = 2000\ \mu g/mL$ (i.e., phosphorous content in the feed tank containing 10% [w/v] corn steep slurry). Based on previous experience *(2)*, V_0, t_d, t_f, and N are set as follows: 50 mL, 2 h, 168 h, and 7 for reactor state (2), respectively, and 3000 mL, 6 h, 168 h, and 7 for reactor state (4), respectively. $V_{FS,\max} = 0.2V_0$ (i.e., the total feed glucose is about 30% [w/v] based on the final culture volume).

After the optimizations introduced in the second section of this article, the feed schemes of glucose and corn steep slurry (phosphorous source) at the start of all subintervals were determined and are listed in Table 4.

Table 4
Optimized Feed Amounts of Dry Glucose Powder (W_{FS}) and Corn Steep Slurry (V_{FPh}, 10% [w/v]) at Start of Each Subinterval, and Culture Volume (V) After Feed Operation in Reactor States (2) and (4), Respectively

	500-mL Shaking flask, 50–60 mL, 160 rpm, and four layers of gauze			5-L Stirred vessel (BioStat B5; BBI), 3.0–3.6 L, 1.5 vvm, and 400 rpm		
t (h)[a]	W_{FS} (g)	V_{FPh} (mL)	V (mL)	W_{FS} (g)	V_{FPh} (mL)	V (mL)
0	—	—	50	—	—	3000
0^+	6.43	1.50	55.07	389.0	9.4	3222
24^+	2.48	0.00	56.46	7.8	0.0	3226
48^+	8.68	0.00	61.28	471.7	0.1	3489
72^+	0.37	0.00	61.48	0.4	0.3	3489
96^+	0.09	0.00	61.53	8.7	0.1	3494
120^+	0.04	0.00	61.55	196.2	0.5	3604
144^+	0.03	0.00	61.56	12.9	0.4	3611

[a]Times with a superscript plus mean the moment just after the feed operations.

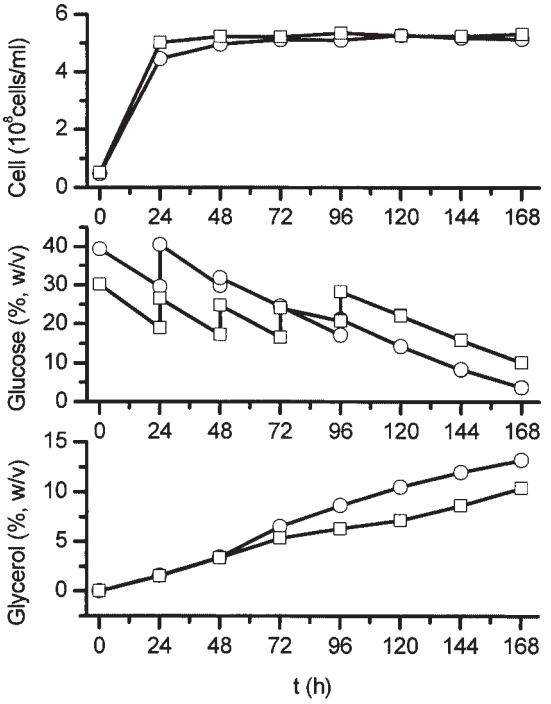

Fig. 4. Comparison between fed-batch process with DPF strategy obtained by constrained global optimization (N = 7) (○) and that with strategy of Yang *(5)* (□) in 500-mL shaking flask (50 mL, 160 rpm, and four layers of gauze).

The optimized strategies were compared with the feed strategy of Yang *(5)* by experiments, and the comparisons of the experimental results are shown in Figs. 4 and 5.

Generally, a relatively higher initial glucose concentration ($S_0 \leq S_{up}$) is more favorable for glycerol formation since in Eq. 3 the second term is the dominant during most of the fermentation process. Both Figs. 4 and 5 suggested that a high pulse-feed operation of glucose should be performed at the start of the fermentation to increase the initial glucose concentration up to the maximum value, 40% (w/v). It was found that the average glycerol yields at h 168 with the optimized strategies proposed were 13.2% (w/v) in reactor state (2) (Fig. 4) and 18.2% (w/v) in reactor state (4) (Fig. 5). Compared with those with the feed strategies of Yang *(5)*, they were improved by 27.0 and 28.2%, respectively. Here the results were just average values of the duplicate experiments, between which most of the relative errors of the experimental data were <5%. However, even if the maximum relative error between the duplicate experiments were close to 10%, the comparisons still showed that the final yield of glycerol fed-batch fermentation could be significantly improved by the suboptimal control strategy employed.

Additionally, comparison of the experimental data and corresponding model predictions are illustrated in Figs. 6 and 7; the experimental cell

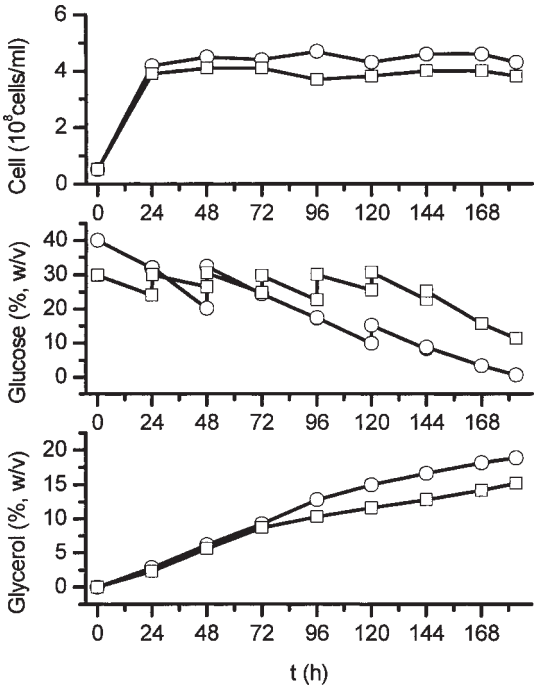

Fig. 5. Comparison between fed-batch process with DPF strategy by constrained global optimization (N = 7) (○) and that with strategy of Yang *(5)* (□) in 5-L stirred vessel (BioStat B5, BBI, Germany; 3–3.6 L; 400 rpm; 1.5 vvm).

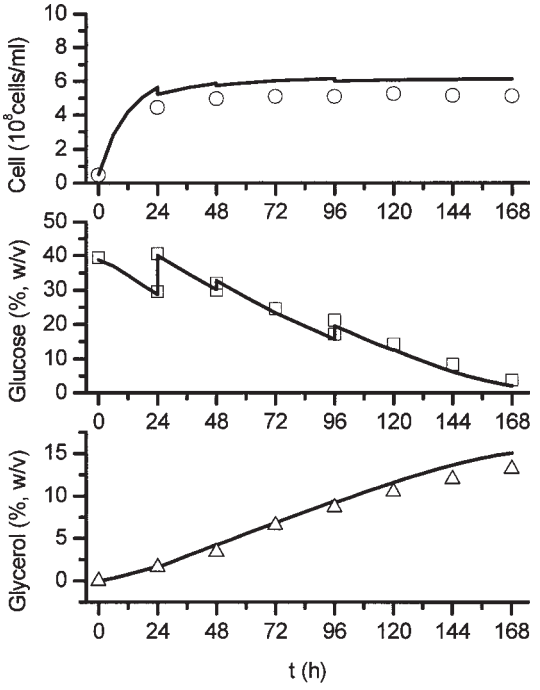

Fig. 6. Comparison between experimental data (○, cell; □, glucose; △, glycerol) and corresponding model predictions of fed-batch process with DPF strategy obtained by constrained global optimization (N = 7) in 500-mL shaking flask (50 mL, 160 rpm, and four layers of gauze).

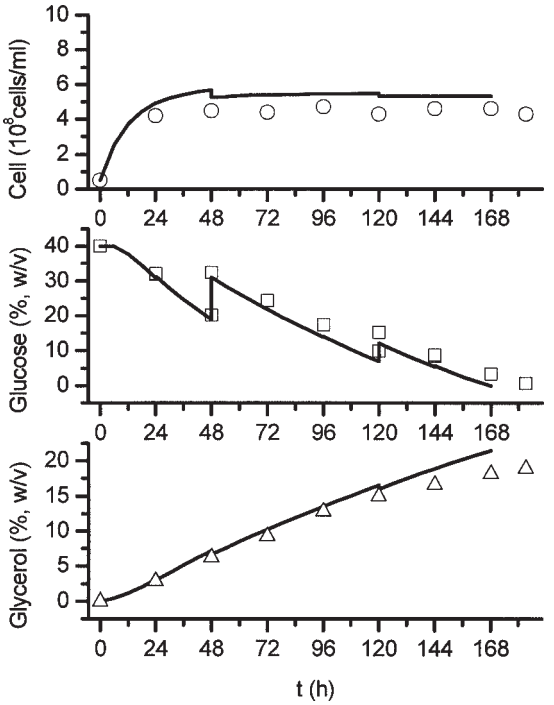

Fig. 7. Comparison between experimental data (○, cell; □, glucose; △, glycerol) and corresponding model predictions of fed-batch process with DPF strategy obtained by constrained global optimization (N = 7) in 5-L stirred vessel (BioStat B5, BBI; 3–3.6 L, 400 rpm, 1.5 vvm).

density and glycerol yield were found somewhat less than those of the model predictions. The possible reason is that the significant and frequent glucose pulse-feeding operation exerted an excess osmotic pressure shock on the yeast, and then resulted in growth inhibition and a decrease in glycerol production. However, the model employed for fed-batch optimization was developed only on the basis of batch experiments, and thus could not predict any changes in the dynamics caused by fed-batch operation. Although the model should be further improved for wider application in the future, the application examples in our study still suggested that the VKP approach was an efficient and promising way to solve the optimization problem in various reactor states or during scale-up processes.

Conclusion

To enable the macrokinetic model proposed in previous work *(2)* to describe flexibly the variable aerobic glycerol fermentation process when the form, scale, and/or operation state such as aeration rate of the reactor (reactor state) are significantly changed, the kinetic parameters were classified into two groups. One group (μ_{max}, K_t, K_O, K_{S1}, K_{IS}, $Y_{X/S}$, m_t, K_{SP}, $Y_{P/S}$, α, β, $Y_{X/Ph}$, K_{S2}) was associated basically with the inherent microscopic bio-

chemical mechanism and cannot be influenced by the macroscopic physical transport process; thus, they are called *invariable kinetic parameters*. The second group (K_{do1}, K_{do2}, K_{Ph1}, K_{Ph2}, and K_{Ph3}) was dependent not only on the microbial reaction mechanism, but also on the physical transport phenomena in reactor and are called VKPs. By reestimating the values of only two key VKPs (K_{do1}, K_{Ph1}), the macrokinetic model could describe well the batch processes in different reactor states. This VKP approach was further applied in model-based optimization of DPF strategies of glucose and corn steep slurry in two scale-down and scale-up glycerol fed-batch processes. The experimental results showed that, compared with the feed strategies determined by experimental optimization in previous work *(5)*, the DPF strategies adjusted according to the VKPs' improved glycerol productivity at least by 27%. The approach proposed in our study also provided a good reference for modeling and optimization of the similar microbial fermentations during scale-up process.

Acknowledgment

We gratefully acknowledge the financial support from China Postdoctoral Science Foundation.

Nomenclature

DPF = Discrete-pulse feed
$fpen$ = Penalty function, dimensionless
J = Objective function (g)
K_{do1} = Constant of dissolved oxygen for cell growth (10^8 cells/mL)
K_{do2} = Constant of dissolved oxygen for glycerol accumulation (10^8 cells/mL)
K_{IS} = Constant for inhibition of glucose in cell growth (g/100 mL)^2
K_O = Ratio of oxygen promotion to cell growth (dimensionless)
K_{Ph1} = Saturation constant for phosphorus for cell growth (μg/mL)
K_{Ph2} = Saturation constant for phosphorus for glucose consumption (μg/mL)
K_{Ph3} = Saturation constant for phosphorus for glycerol production (μg/mL)
K_{S1} = Contois constant for glucose for cell growth (g/10^{10} cells)
K_{S2} = Saturation constant for glucose for phosphorous consumption (g/100 mL)^2
K_{SP} = Coefficient of glycerol as a carbon source compared with glucose (dimensionless)
K_t = Attenuation constant for culture time for cell growth (h)
m_t = Total maintenance coefficient of both glycerol and glucose (g/10^{10} cells)
N = Total number of the subintervals (dimensionless)
P = Mass concentration of glycerol (g/100 mL), i.e., (% [w/v])

Pen_S = Penalty coefficient for constraint on glucose process concentration (dimensionless)
Pen_{Sf} = Penalty coefficient for constraint on final glucose concentration (dimensionless)
Pen_{VF} = Penalty coefficient for constraint on total feeding volume (dimensionless)
Ph = Concentration of phosphorus (μg/mL)
Ph_{FPh} = Phosphorous concentration in feed tank of corn steep slurry (μg/mL)
Ph_{FS} = Phosphorous concentration in glucose feed tank (μg/mL)
S = Mass concentration of glucose (g/100 mL), i.e., (% [w/v])
S_0 = Initial mass concentration of glucose (g/100 mL), i.e., (% [w/v])
S_{FS} = Glucose concentration in glucose feed tank (g/100 mL), i.e., (% [w/v])
t = Culture time (h)
V = Culture volume (mL)
V_{FPh} = Feed volume of corn steep slurry (mL)
V_{FS} = Feed volume of glucose (mL)
W_{FS} = Feed amount of dry glucose powder (g)
X = Cell numeration (10^8 cells/mL)
$Y_{P/S}$ = Yield coefficient of glycerol production for glucose consumption, glycerol per glucose (g/g)
$Y_{X/Ph}$ = Yield coefficient of cell production for phosphorous consumption, cell number per phosphorus (10^8 cells/μg)
$Y_{X/S}$ = Yield coefficient of cell production for glucose consumption, cell number per glucose (10^{10} cells/g)

Greek

α = Glycerol yield constant associated with cell growth (10^{-10} g/cell)
β = Modified constant associated with cell concentration (10^{-8} mL/[cell·h])
μ = Specific growth rate (h^{-1})
μ_{max} = Maximum specific growth rate (h^{-1})

Subscripts

0 = Initial state of fed-batch fermentation
end = Final state of glucose concentration
f = Final state of fed-batch fermentation
i = Sequence number of subintervals ($1 \le i \le N$)
low = Lower limit
max = Maximum value or upper limit
up = Upper limit

References

1. Zhuge, J. and Fang, H. Y. (1994), *Food Ferment. Ind. (China)* **4,** 65–70.
2. Xie, D.-M. (2000), PhD thesis, Institute of Chemical Metallurgy, Chinese Academy of Sciences, Beijing, P. R. China.
3. Fan, Z.-L. (1996), MSc thesis, Institute of Chemical Metallurgy, Chinese Academy of Sciences, Beijing, P. R. China.
4. Sun, H.-W. (1997), MSc thesis, Institute of Chemical Metallurgy, Chinese Academy of Sciences, Beijing, P. R. China.
5. Yang, Y.-O. (1999), MSc thesis, Institute of Chemical Metallurgy, Chinese Academy of Sciences, Beijing, P. R. China.
6. Vijaikshore, P. and Karanth, N. G. (1987), *Biotechnol. Bioeng.* **30,** 325–328.
7. Johnson, A. (1987), *Automatica* **23(6),** 691–705.
8. Modak, J. M., Lim, H. C., and Tayeb, Y. J. (1986), *Biotechnol. Bioeng.* **28,** 1396–1407.
9. Lim, H. C., Tayeb, Y. J., and Modak, J. M. (1986), *Biotechnol. Bioeng.* **28,** 1408–1420.
10. Xie, D.-M., Liu, D.-H., Zhu, H.-L., and Liu, T.-Z. (2001), *Appl. Biochem. Biotechnol.* **95,** 103–112.
11. Moser, A. (1988), *Bioprocess Technology: Kinetics and Reactors* (translated by Manor, P.), Springer, New York.
12. Gill, P. E. and Murray, W. (1974), in *Numerical Methods for Constrained Optimization*, Academic, New York.
13. Ye, Q.-K. and Wang, Z.-M. (1986), *Computational Methods for Optimization and Optimal Control*, Science Press, Beijing, Chap. 7, pp. 233–271.
14. Box, M. J. (1965), *Comput. J.* **8,** 42–52.
15. Xu, S.-L. (1997), in *Collection of QBASIC Programs for Numerical Computation*, Tsinghua University Press, Beijing, Chap. 12, pp. 402–407, 420–427.
16. Sahoo, D. K. and Agarwal, G. P. (2001), *Process Biochem.* **36,** 839–846.
17. Neish, A. C. (1954), *Analytical Methods for Bacterial Fermentation*, 2nd rev., Bulletin no. 25292, National Research Council of Canada, Ottawa, Canada.
18. Ashworth, M. F. R. (1979), *Analytical Methods for Glycerol*, Academic, New York.
19. Murphy, J. and Riley, J. P. (1962), *Anal. Chim. Acta* **27,** 31–36.